Fermilab

Fermi National Accelerator Laboratory
P.O. Box 500 • Batavia, Illinois • 60510

TD - 03 - 031
March 7, 2003

Analysis of Splice Test Configuration (HFDA-03B)

Deepak Chichili, Vadim Kashikhin, and Alexander Zlobin

The goal is to use HFDA-03A mirror magnet coil and modify it to test the splice joints in a configuration similar to that of in a magnet. The two RE shunts will be unsoldered and in their place new leads will be soldered. Furthermore, the turns will be cut at the RE to separate the mid-plane turn from the rest of the coil. In essence we will be testing four Nb_3Sn – NbTi splice joints connected in series. However, there will be one NbTi – NbTi splice joint between the second and third Nb_3Sn-NbTi splice joint. The coil will then be assembled with the iron mirror in vertical iron yoke gap configuration similar to the mirror magnet.

Magnetic Analysis

Since the splices to Nb_3Sn cables will be made in the magnet straight section – end fields from the NbTi leads can be neglected. In this case, 2D calculation of the magnetic field provides necessary information on the cable parameters. Fig. 1 shows OPERA 2D model used for this purpose. The direct current flows through the mid-plane cable of the outer layer and returns through the mid-plane cable of the inner layer. The model does not show other coil turns, which are electrically disconnected and thus has no effect on the magnetic field.

The splice load line and transfer function are shown in Fig. 2. The transfer function remains constant (equal to 0.0685 T/kA) up to 30 kA current. At the power supply limit of 20 kA, the maximum field in the splice is 1.37 T. The peak field is at the inner surface of the outer-layer cable. The maximum field in the inner-layer cable is about 3 % less at the same current.

The cable quench field and current were parametrically derived from the superconductor properties as shown in Figs. 3-4 for both Nb_3Sn and NbTi cables. Fig. 4 shows the quench parameters for one NbTi cable made of 34 SSC inner strands with 0.808 mm diameter and copper to non-copper ratio of 1.3. The Nb_3Sn cable with an expected short sample limit of 1800 A/mm^2 at 12 T and 4.2 K would have the quench field of 4.9 T at 74.3 kA quench current that is far above the power supply limit. The short sample limit of NbTi SSC strand is around 2750 A/mm^2 at 5 T and 4.2 K, which leads to the quench field of 2.8 T at 41.0 kA current.

A second thermal cycle is also planned with one cable disconnected and one was connected to the power supply. Figure 5 shows the field distribution in this case and Figures 6-7 present load line and short sample limit. Due to smaller field on the cable, the expected quench current is ~ 14 % higher than in the previous case when both cables are powered. The transfer function is non-linear already at low fields due to saturation of the iron yoke with the unbalanced current from single cable.

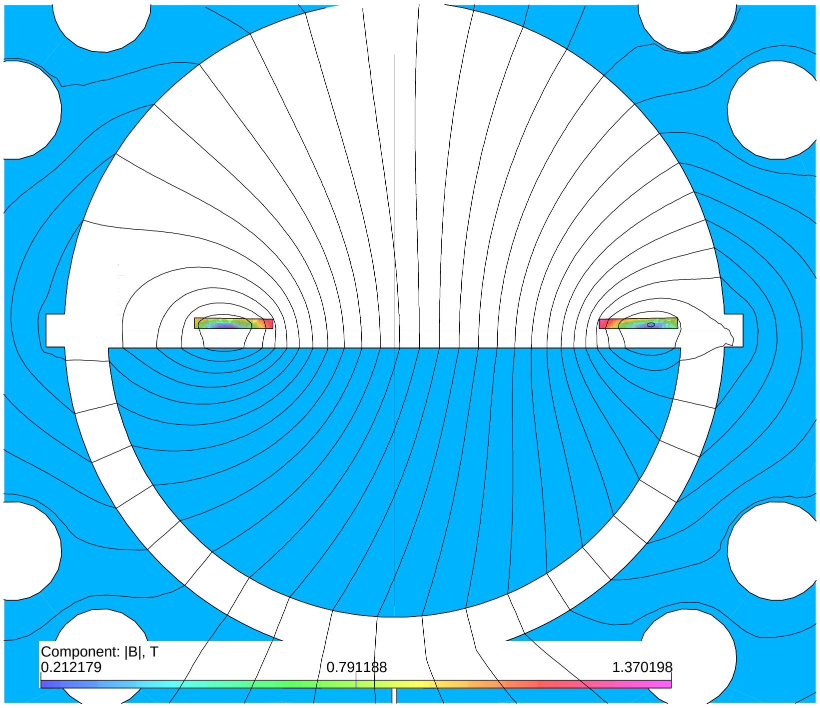

Fig. 1: Field map in the splice test configuration.

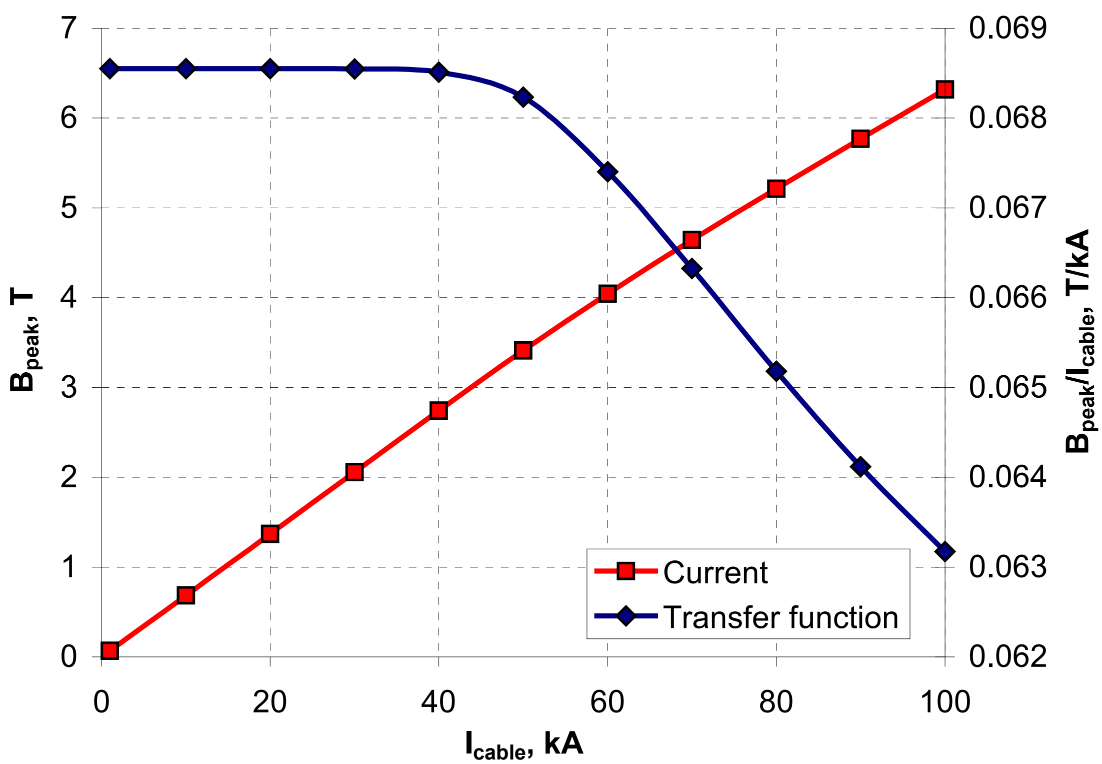

Fig. 2: Peak field and transfer function as functions of the current.

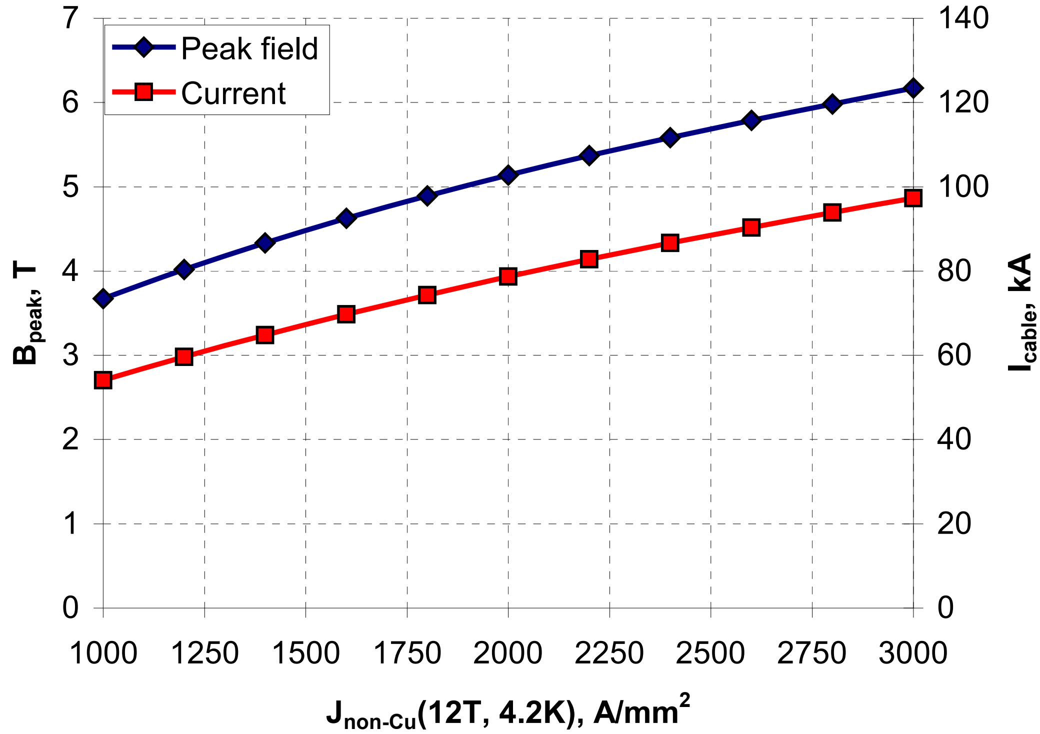

Fig. 3: Quench field and current for the Nb_3Sn cable.

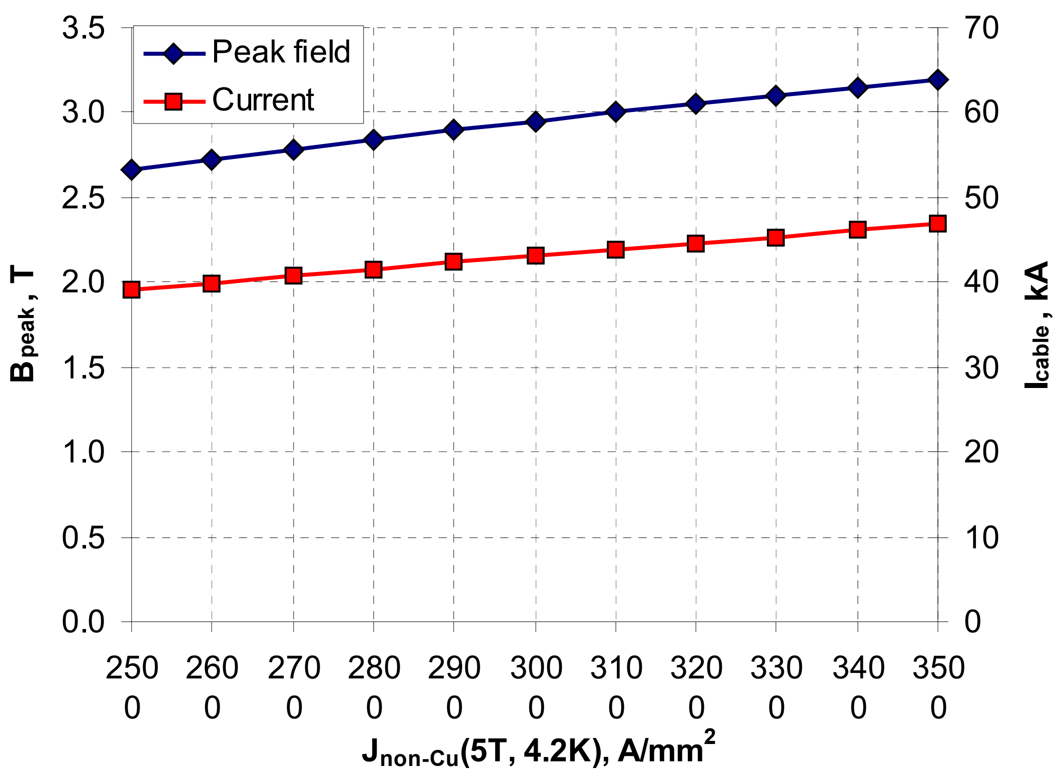

Fig. 4: Quench field and current for the NbTi cable.

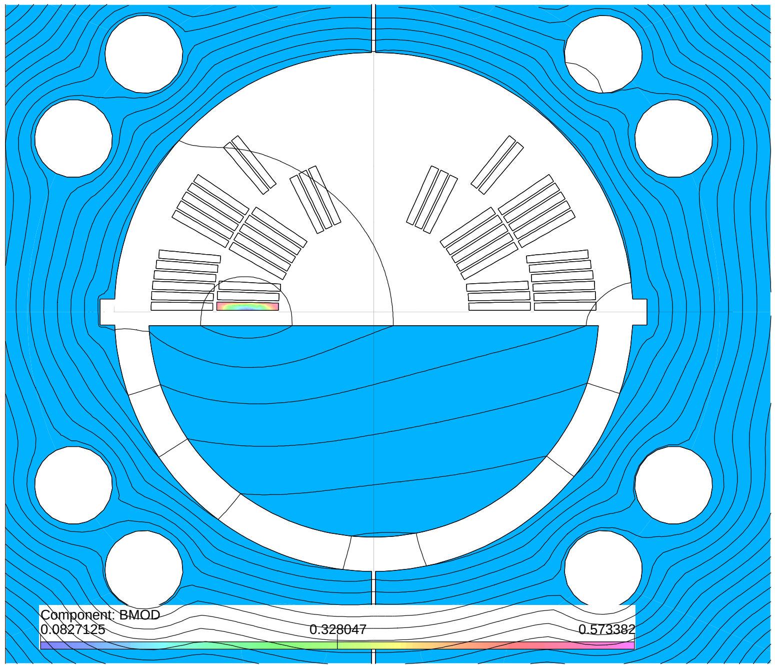

Fig. 5: Field map in the single cable test.

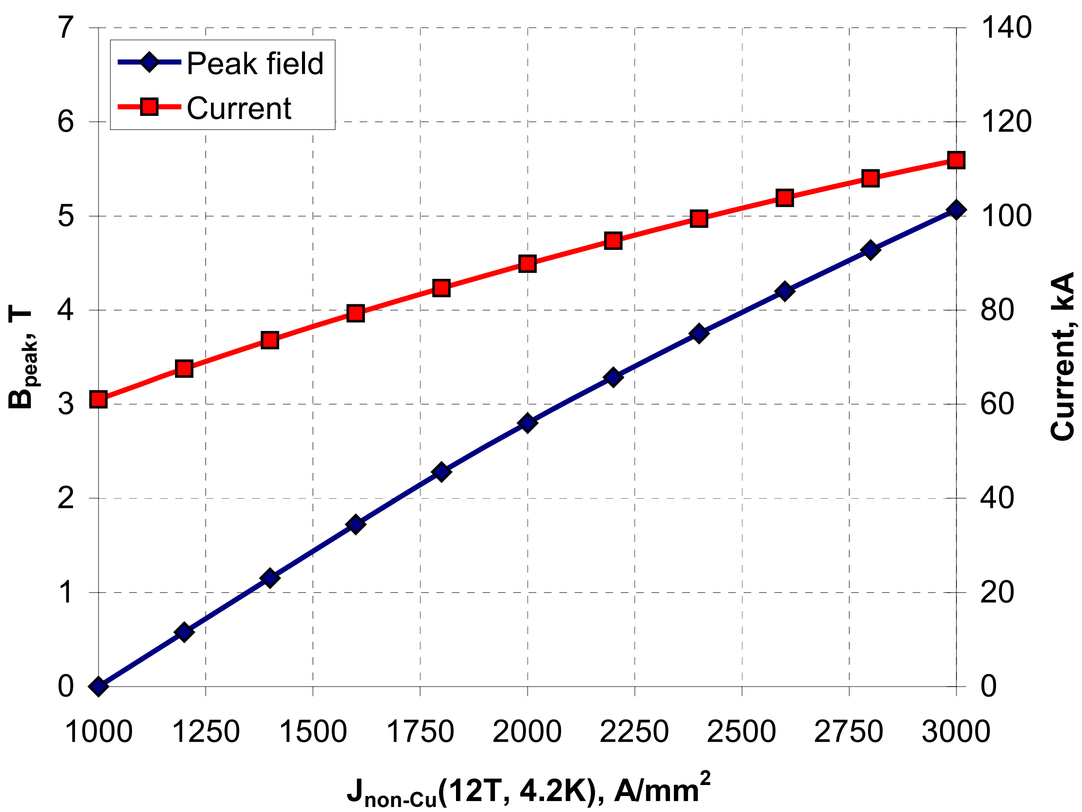

Fig. 6: Peak field and transfer function as functions of the current.

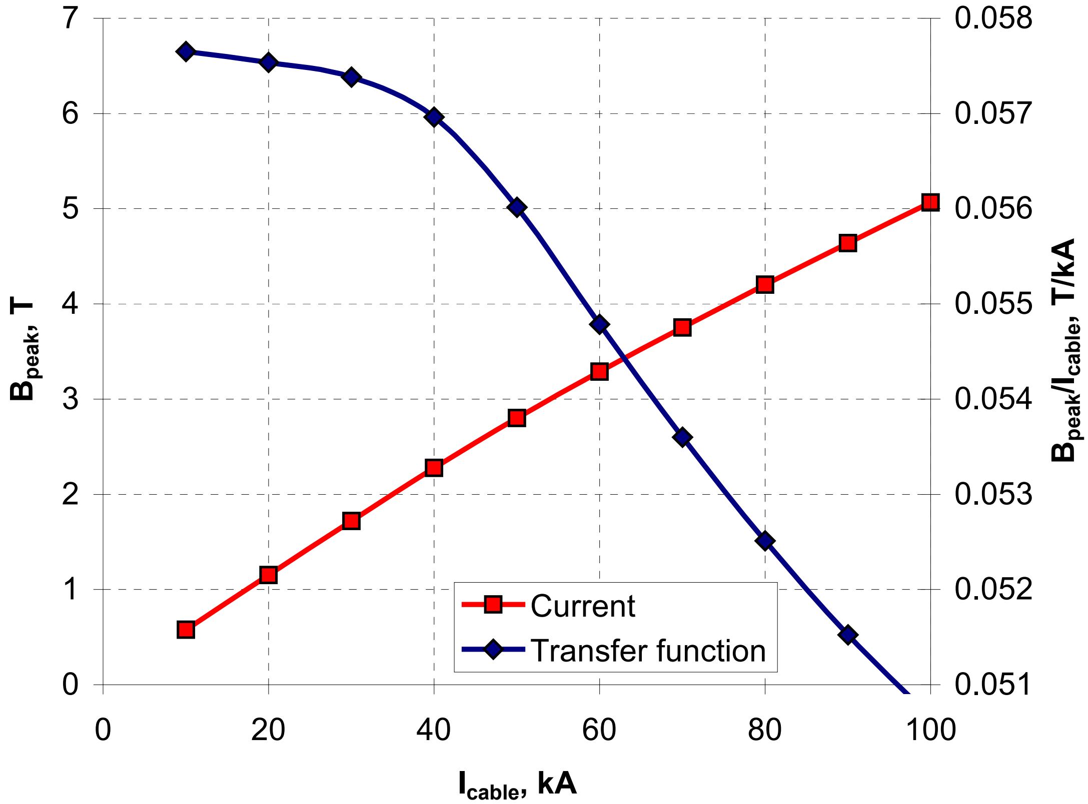

Fig. 7: Quench field and current for the Nb_3Sn cable.

Mechanical Analysis

Finite element analysis using ANSYS was carried out to estimate the stresses in the coil and in other structural components. The following are the initial conditions for which the results are reported in this note. The interference/gap's between various components were obtained after several iterations and we believe are optimal for the proposed splice-test configuration.

- ⇒ Radial interference between coil and spacer is 0.05 mm. This will increase the pre-stress in the coil during yoking/clamping operation thereby reducing the amount of effort with tightening the bolts on the skin.
- ⇒ Radial gap between iron mirror and spacer is 0.075 mm. This will decrease the load on the iron mirror during assembly. The gap would allow the assembly to transfer the load to the coil first before contacting the iron mirror.
- ⇒ Azimuthal interference between pole extension and spacer is 0.05 mm. This will ensure that the spacer is in compression and in contact with the coil and the iron yoke at all stages of the magnet operation.
- ⇒ Interference between clamp and iron yoke is 0.25 mm. This delivers the pre-stress to the coil during yoking/clamping.

⇒ Equivalent weld shrinkage due to bolted skin is 0.025 mm. This step will restore some of the pre-stress in the coil lost due to the spring back of the aluminum clamp after releasing the pump pressure.

Analysis was done for different stages of magnet assembly/operation – yoking @ 8000 pump-Psi, after clamping, after skinning, 4.2 K, 0 A and 4.2 K, 20 A. The last step is irrelevant in the splice-configuration, however the data is included in the note for future use. Typically during yoking, the pump pressure would be increased slowly until the gap between the yoke halves reaches nominal size. To understand this operation pre-stress in the coil and in the spacer was estimated at incremental loads that match the applied pump pressure during yoking.

The rest of the note shows plots of estimated pre-stress in the coils, radial and azimuthal displacement of coil assembly, and azinuthal stress in the spacer at various locations. Note again that for this particular test, only the mid-plane data up to 4.2 K, 0 A is relevant. However VMTF has recently developed a new capacitance gauge readout system and the coil will be instrumented to read out stresses both at the mid-plane and in the pole region. So the plots include the pole data as well.

Fig. 8 shows the ANSYS model for the vertical yoke gap design with applied boundary conditions.

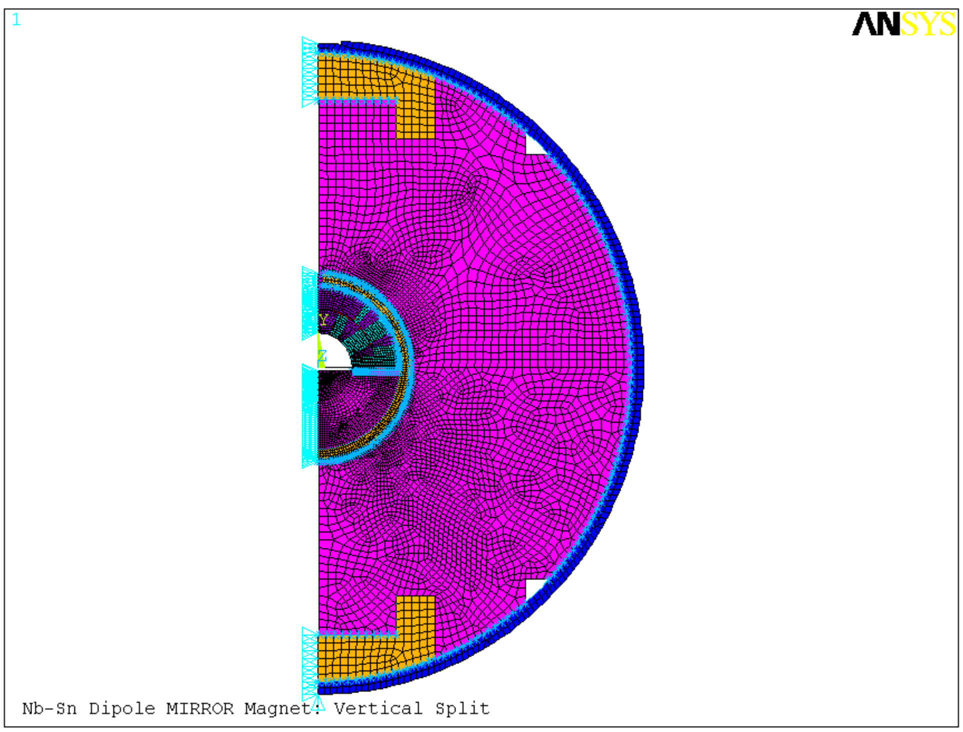

Fig. 8(a): ANSYS model for the vertical-split approach

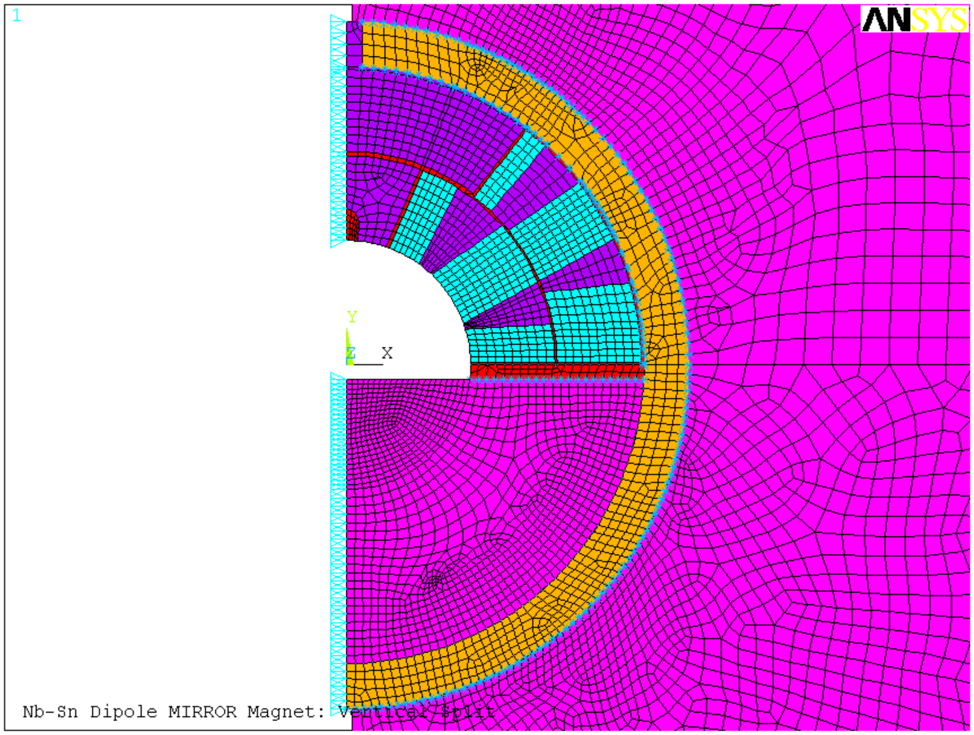

Fig. 8(b): Close up view of the ANSYS model.

Fig. 9 shows the peak azimuthal stress in the coil at various stages. Note that the location of the peak stress is different at different stages. During yoking it is at the edge of the outer mid-plane, after clamping, skinning and at 4.2K, 0A it is at the inner pole region and at 4.2 K, 20 A it is in the outer mid-plane region. The maximum peak stress is about 105 MPa, seen during the excitation.

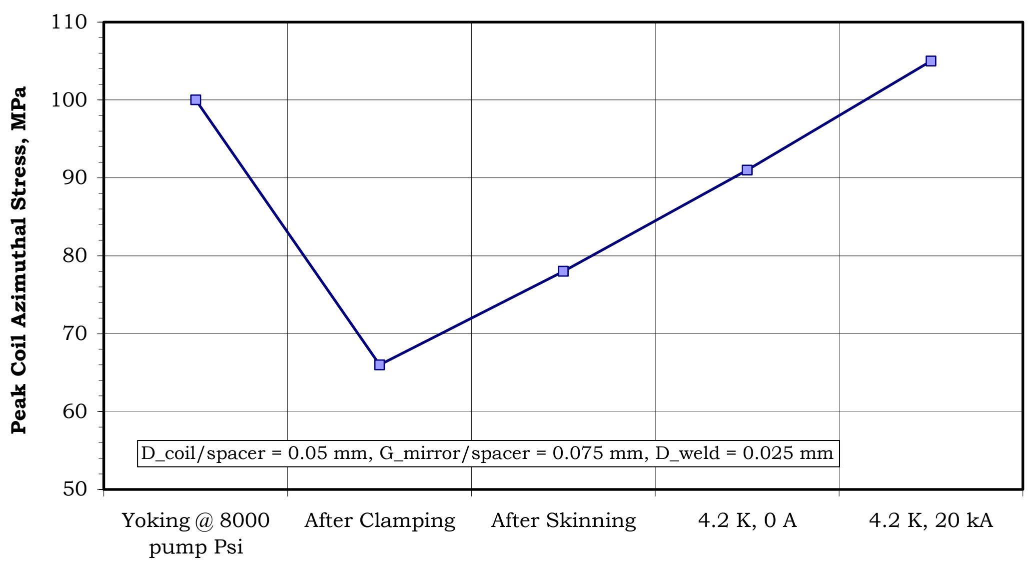

Fig. 9: Estimation of the peak azimuthal stress in the coil

The capacitance gauges however measure the average stress along the width of the cable at a given location. Fig. 10 shows the average stresses at various locations of the coil. The mid-plane turn, which is of interest for splice test, sees a maximum average stress of about 62 MPa during cool down.

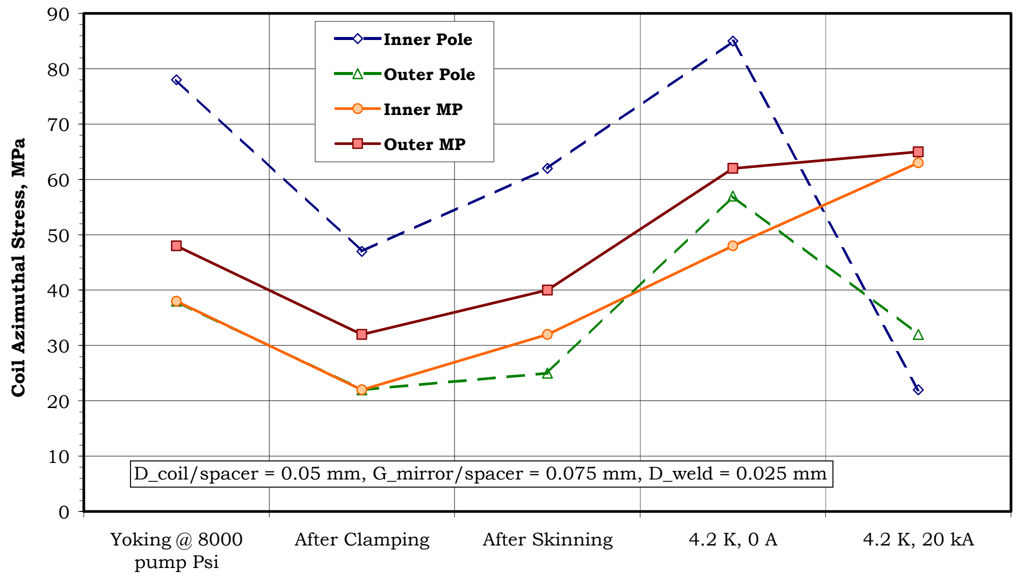

Fig. 10: Estimation of the average azimuthal stress in the coil

Resistive gauges will be used to measure the azimuthal stress in the spacer both at the pole and mid-plane locations. Fig. 11 gives the estimated stress in the spacer at various stages of magnet assembly and operation. Note that the stress in the spacer pole region near the coil is different from that of near iron mirror due to different contact conditions.

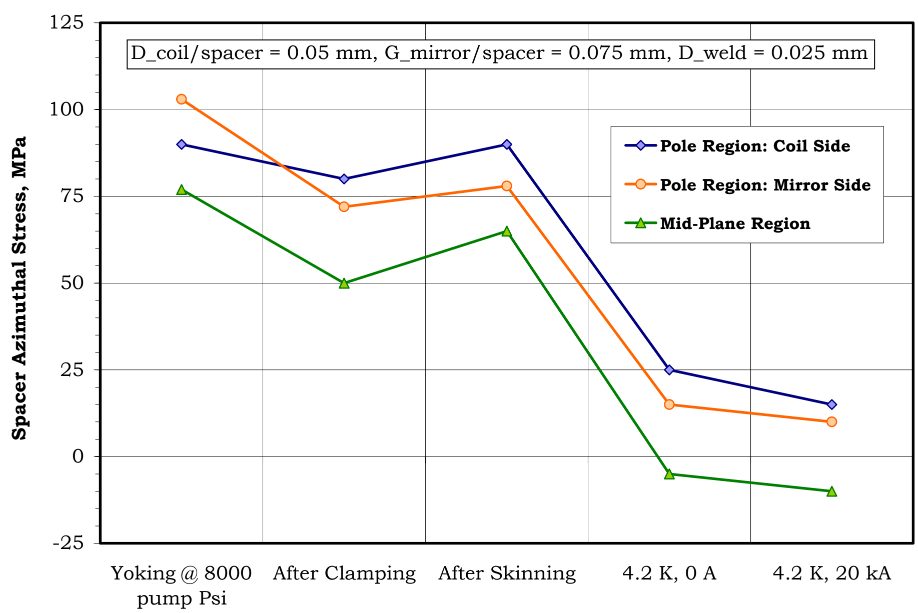

Fig 11: Azimuthal stress in the spacer at various stages of the magnet assembly/operation.

It is also important to understand the displacement of the coil assembly during these stages. The radial and azimuthal displacements near the inner pole and mid-plane region are shown in Figs. 12 and 13. Zero displacement represents the nominal position of the coil before the assembly process. The assembly moves radially inwards by about 0.1 mm during cool down. On excitation, the motion is limited to 0.04 mm and furthermore the coil aperture returns to circle configuration.

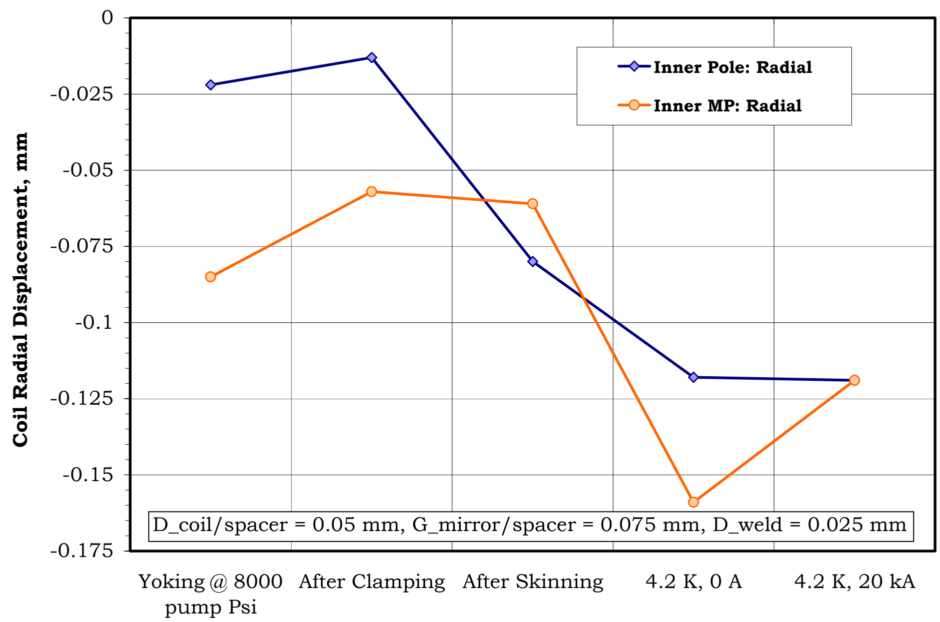

Fig. 12: Radial displacement in the coil inner pole and mid-plane region.

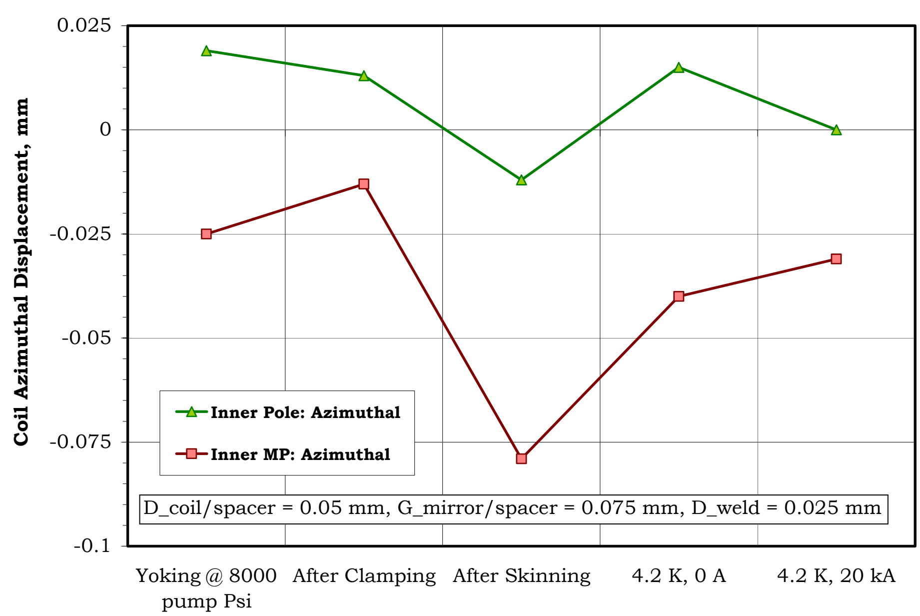

Fig. 13: Azimuthal displacement in the coil inner pole and mid-plane region.

Finally the evolution of stress in the coil and in the spacer during yoking operation is shown in Figs. 14 and 15. The inner pole region sees the maximum stress during yoking operation. For the upcoming splice test, we will not be able to put the capacitance gauge in the inner pole region. It might be good idea to start thinking about implementing this in the future magnets.

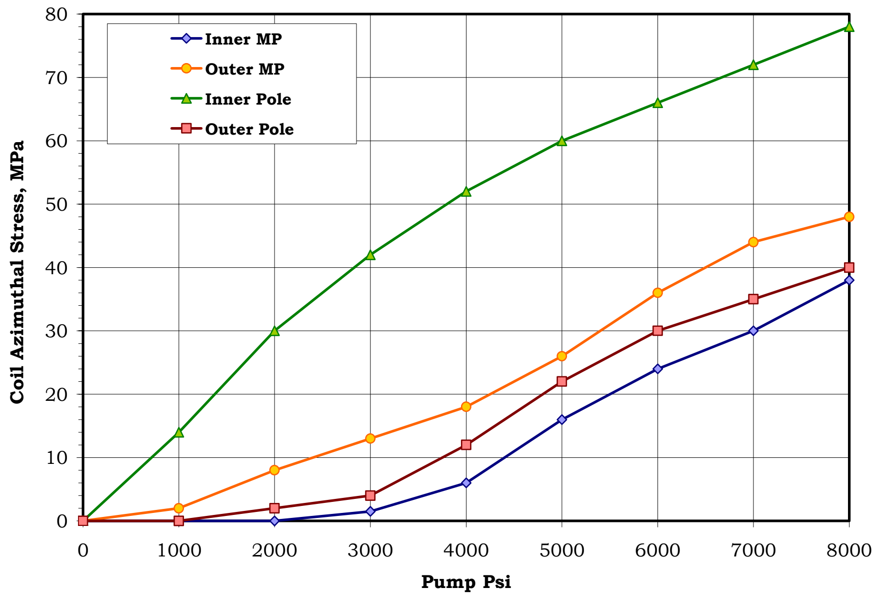

Fig. 14: Evolution of coil stress during yoking operation

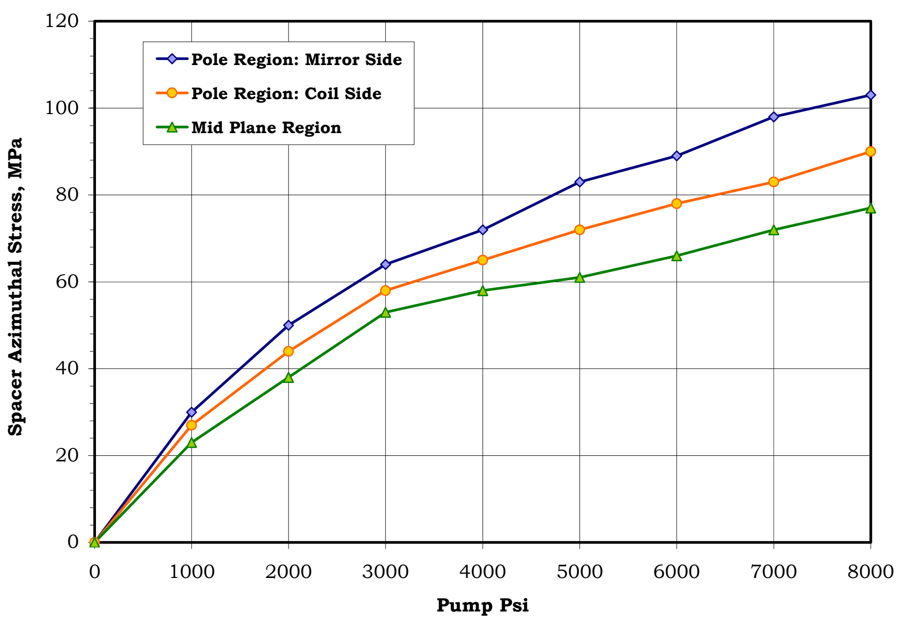

Fig. 15: Evolution of spacer stress during yoking operation

The contour plots, which illustrate the distribution within the coil assembly, are shown in the Appendix.

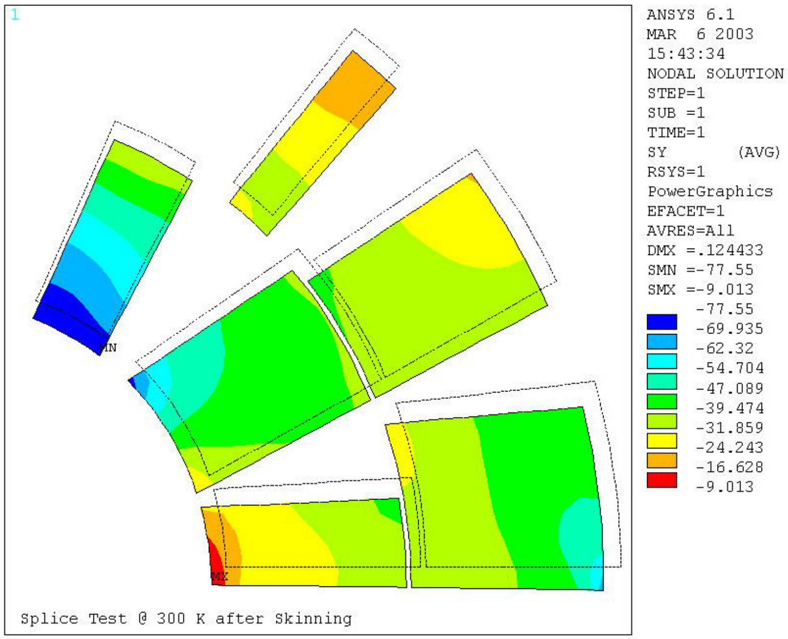

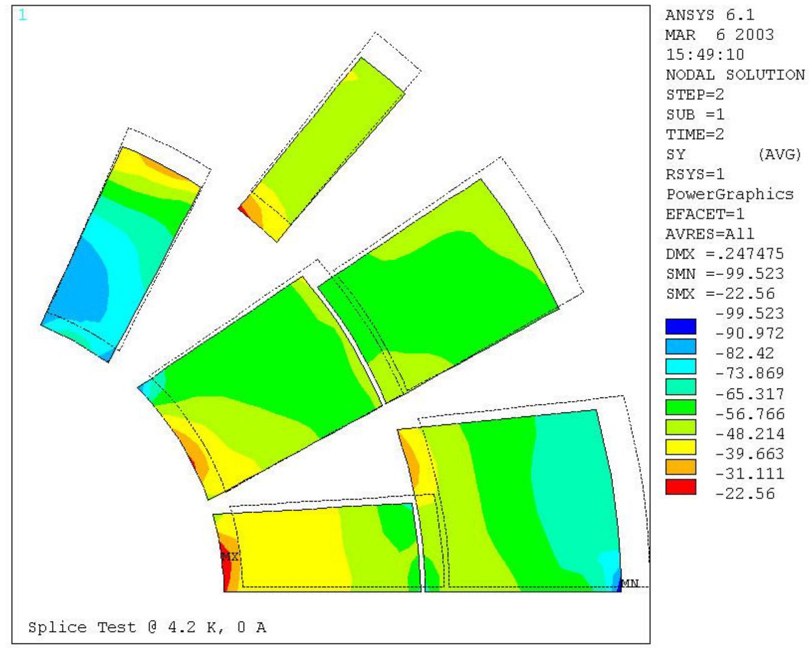

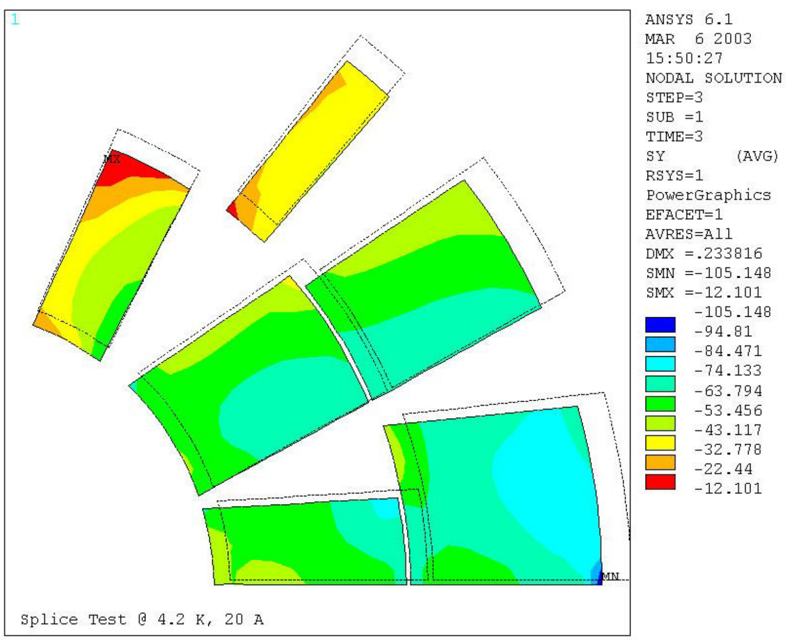

Contour plots showing the azimuthal stress distribution in the coil after skinning, 4.2 K, 0A and 4.2 K, 20A

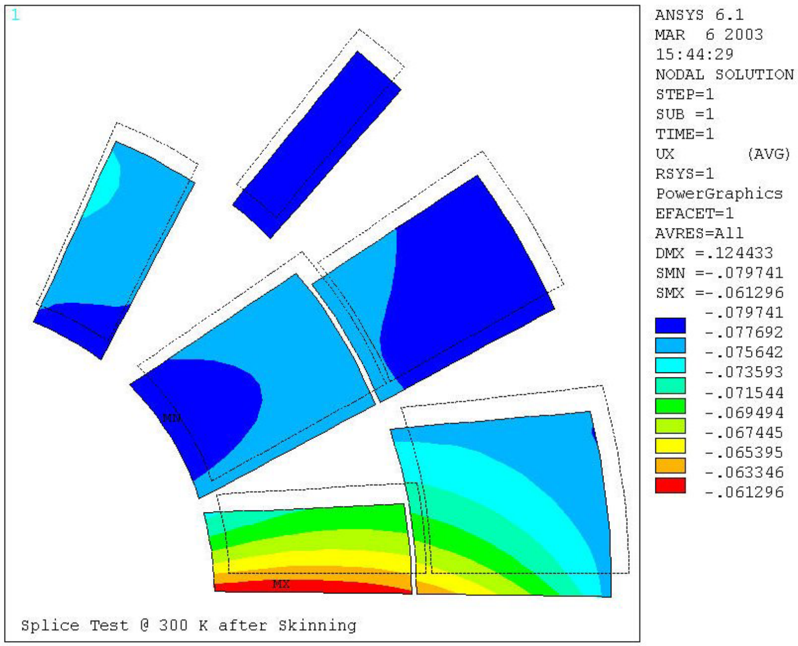

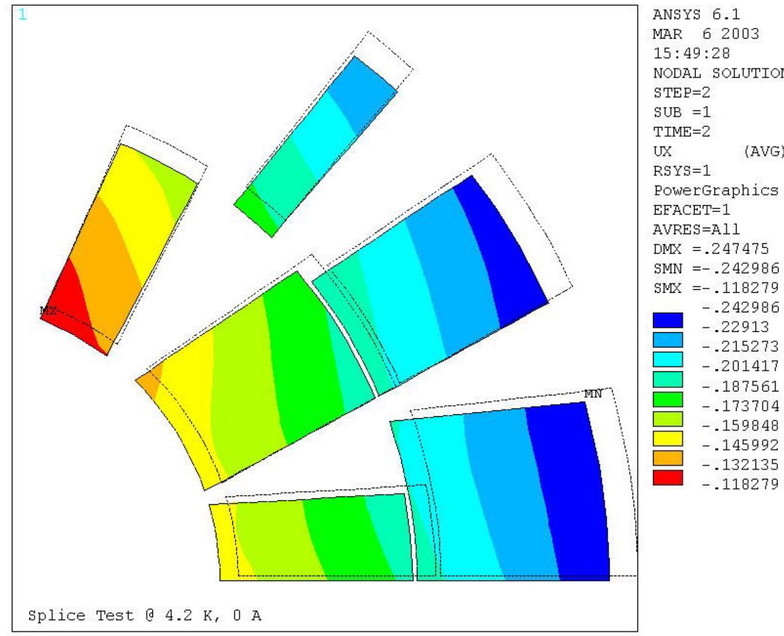

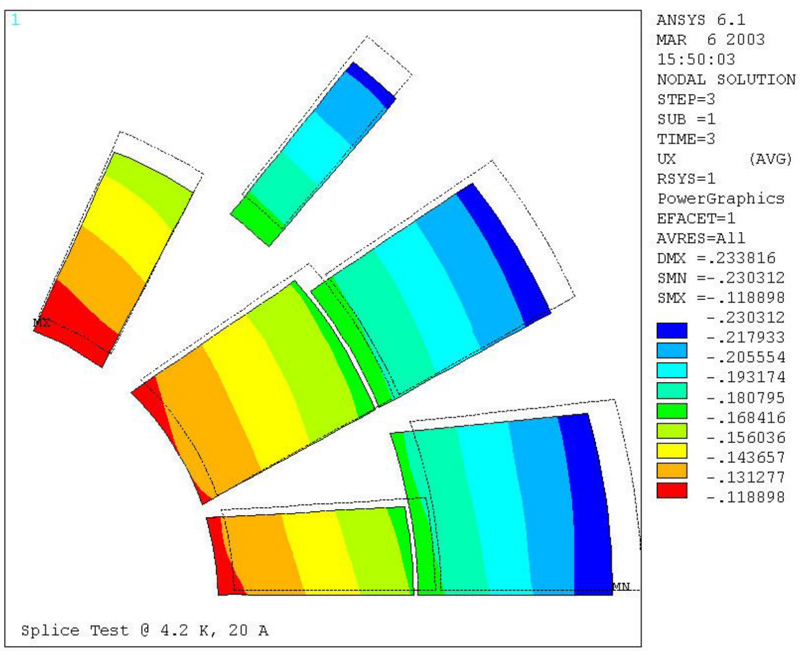

Contour plots showing the radial displacement in the coil after skinning, 4.2 K, 0A and 4.2 K, 20A